HIPPOCAMPUS 16:161–173 (2006)

Input Source and Strength Influences Overall Firing Phase of Model Hippocampal CA1 Pyramidal Cells During Theta: Relevance to REM Sleep Reactivation and Memory Consolidation

Victoria Booth[1,2*] and Gina R. Poe[1,3]

ABSTRACT: In simulation studies using a realistic model CA1 pyramidal cell, we accounted for the shift in mean firing phase from theta cycle peaks to theta cycle troughs during rapid-eye movement (REM) sleep reactivation of hippocampal CA1 place cells over several days of growing familiarization with an environment (Brain Res 855:176–180). Changes in the theta drive phase and amplitude between proximal and distal dendritic regions of the cell modulated the theta phase of firing when stimuli were presented at proximal and distal dendritic locations. Stimuli at proximal dendritic sites (proximal to 100 μm from the soma) invoked firing with a significant phase preference at the depolarizing theta peaks, while distal stimuli (>290 μm from the soma) invoked firing at hyperpolarizing theta troughs. The input location-related phase preference depended on active dendritic conductances, a sufficient electrotonic separation between input sites and theta-induced subthreshold membrane potential oscillations in the cell. The simulation results predict that the shift in mean theta phase during REM sleep cellular reactivation could occur through potentiation of distal dendritic (temporo-ammonic) synapses and depotentiation of proximal dendritic (Schaffer collateral) synapses over the course of familiarization. © 2006 Wiley-Liss, Inc.

KEY WORDS: place cells; simulation; learning; Schaffer collateral; temporo-ammonic

INTRODUCTION

During rapid-eye movement (REM) sleep and non-REM sleep episodes following exploration of an environment, hippocampal CA1 place cells replay their firing in the same sequential order as observed during waking exploration (Wilson and McNaughton, 1994; Skaggs and McNaughton, 1996; Louie and Wilson, 2001; Lee and Wilson, 2002). Replay of place cell firing ensembles during sleep is thought to contribute to the consolidation of the associated memories within the hippocampus and to their transfer to neocortical long-term stores (reviewed in Hobson and Pace-Schott (2002) and Ribeiro and Nicolelis (2004)). During REM sleep, reactivated firing occurs on a similar timescale as during exploration (Louie and Wilson, 2001), and the hippocampal theta rhythm (5–10 Hz), which is critical to learning (Mizumori et al., 1990; Givens, 1996; Rashidy-Pour et al., 1996), resumes or exceeds active waking strength (Vanderwolf et al., 1977). Phase precession of hippocampal place cell firing relative to the theta rhythm also recurs as in waking exploration (Poe et al., 2000; Louie and Wilson, 2001; Harris et al., 2002). As an animal becomes familiar with an environment over several days, a shift occurs in the overall phase of theta at which cells predominantly fire during REM reactivation (Poe et al., 2000). In the first 2 days of REM sleep following exploration of an initially novel environment, the majority of spikes occurred near the depolarizing peak of the theta rhythm, as during waking. But over the following days as the rat became more familiar with the environment, the mean theta firing phase during REM shifted. By the 5th day, cells fired primarily near the hyperpolarizing trough of the theta cycle. Place cell firing in the hyperpolarizing theta troughs during REM replay may facilitate depotentiation of synaptic connections involved in place cell ensembles encoding familiar environments to prevent saturation of the network and allow encoding and storage of new information (Poe et al., 2000).

The neural mechanisms generating the shift in mean firing phase during REM reactivation have not been determined. In this article, we present a simulation study to investigate mechanisms that can account for this shift in mean firing phase from the theta peak to the theta trough as observed in REM replay of place cells over the course of familiarization.

The amplitude and phase of extracellularly recorded theta waves display a transition through the layers of CA1 from stratum oriens (above the cell layer) to the deep stratum lacunosum moleculare (SLM) Buzsaki (2002), Gillies et al. (2002), and Kowalczyk and Konopacki, (2002). Specifically, when the somatic membrane potential is most hyperpolarized (at the trough of the cycle), the distal dendritic membrane potential is most depolarized. Thus, the somatic membrane potential

[1] **Department of Anesthesiology, University of Michigan, Ann Arbor, Michigan 48109;** [2] **Department of Mathematics, University of Michigan, Ann Arbor, Michigan 48109;** [3] **Department of Molecular and Integrative Physiology, University of Michigan, Ann Arbor, Michigan 48109**
Grant sponsor: National Science Foundation; Grant numbers: DBI-0340687, DMS-0315862; Grant sponsor: National Institute of Mental Health; Grant numbers: MH060670, MH076280; Department of Anesthesiology.
*Correspondence to: Victoria Booth, Department of Anesthesiology, 7433 Medical Science Building I, 1150 West Medical Center Drive, Ann Arbor, MI 48109-9332. E-mail: vbooth@umich.edu
Accepted for publication 16 October 2005
DOI 10.1002/hipo.20143
Published online 12 January 2006 in Wiley InterScience (www.interscience.wiley.com).

oscillates out of phase with distal dendritic membrane potentials. In addition, recordings from the soma and distal (SLM) dendrites of CA1 pyramidal cells reveal that activation of the theta rhythm generally hyperpolarizes the somatic membrane while it simultaneously depolarizes the dendritic membrane (Kamondi et al., 1998).

In this simulation study, we investigated how the somato-dendritic shift in the theta rhythm can differently affect the mean theta phase of firing in response to proximal and distal dendritic synaptic inputs. Using a realistic model of a CA1 pyramidal cell, we injected input at proximal sites consistent with locations of Schaffer collateral (SC) input in the stratum radiatum (SR) layer of CA1. Distal input was injected in the SLM layer where the direct, temporo-ammonic pathway (TA) from layer III of the entorhinal cortex (EC) synapses at dendrites of CA1 pyramidal cells. The simulated rhythmic theta drive to the model cell induced antiphase subthreshold membrane potential oscillations in the proximal and distal dendritic regions. The results propose that in the presence of the theta drive, excitatory input at SC-CA1 synaptic sites preferentially generates firing near the depolarized peak of the theta cycle while excitatory input at TA-CA1 synaptic sites preferentially generates firing in the theta trough.

As expected, the effect of the somato-dendritic shift in the theta rhythm on firing phase decreases as input strengths become very large. In this case, the cell would fire at all theta phases regardless of the input location. As such, our simulation results concentrate on investigating constraints on input and theta drive characteristics that yield statistically significant mean firing phases (in contrast to random or uniform phase distributions) and statistically significant differences in mean firing phases when input locations vary.

A prediction of our simulation results is that the shift in mean firing phase from the theta peak to the theta trough, as observed in REM replay of place cells over the course of familiarization, is generated by a change in the relative strengths of proximal and distal dendritic synaptic inputs. Specifically, the simulation results support the hypothesis that depotentiation at SC-CA1 synapses and potentiation at TA-CA1 synapses during learning changes the mean theta phase profile, a phenomenon which is unmasked under REM sleep reactivation conditions and facilitated by such REM-specific reactivation. In the Discussion, we briefly summarize results from the literature that further support this hypothesis.

MODEL

We used a realistic model of a CA1 pyramidal cell developed by Migliore et al. (1999), (Fig. 1A). This model has been used in several studies, including investigations of the role of the potassium A-type conductance on the back-propagation of action potentials (Migliore et al., 1999), the integration of subthreshold synaptic inputs (Migliore, 2003), and the pharmacological modulation of dendritic excitability (Poolos et al., 2002). The model runs via the NEURON simulation program (Hines and Carnevale, 1997) and is publicly available under the ModelDB section of the Senselab database (http://senselab.ale.med.edu).

The active currents included in the model are an inward sodium current, a potassium delayed-rectifier current, an A-type potassium current I_A, and a hyperpolarization-activated, nonspecific cation current, I_h. All currents are modeled in the Hodgkin–Huxley formalism and activation kinetics and parameter values are based on experimental measurements of CA1 pyramidal cells (see Migliore et al. (1999) for model equations and Poolos et al. (2002) for parameter values used). In particular, both I_A and I_h are nonuniformly distributed along the apical dendrites; their maximal conductances increase linearly with distance from the soma. In dendritic compartments more distal than 100 μm from the soma, the activation curves for I_A and I_h are shifted by -10 and -8 mV, respectively. The distribution of these currents becomes relevant during REM sleep when neurotransmitters that would boost I_h currents and suppress I_A currents are uniquely absent (reviewed in Pace-Schott and Hobson (2002), see Discussion). Sodium and potassium delayed-rectifier currents are uniformly distributed. The model does not contain calcium or calcium-dependent currents. This simplification of the model, however, does not qualitatively affect our results. All compartments more distal than 500 μm from the soma or with a diameter smaller than 0.5 μm are modeled as passive. The model with the parameter values used here, as in Poolos et al. (2002), accurately replicated experimentally recorded firing of CA1 pyramidal cells in vitro in response to current steps injected in the soma and dendrites (Poolos et al., 2002).

The theta rhythm drive to the cell was modeled as in Harris et al. (2002) as 10 Hz sinusoidally-varying conductances inserted in a proximal compartment (100 μm from soma center) and a distal compartment (328 μm from soma center) along the main apical dendritic shaft. The proximal theta drive current was inhibitory (reversal potential -80 mV) with a maximal conductance varying sinusoidally between 2 and 8 nS (Fig. 1B, solid trace). The distal theta drive current was excitatory (reversal potential 0 mV) and its maximal conductance varied sinusoidally between 0.7 and 2.8 nS (Fig. 1B, dashed trace). The theta rhythm frequency and duration of the generic excitatory input (see later) were chosen to elicit firing over 5–7 theta cycles as is observed, on average, during a place cell firing episode during waking and REM sleep (Poe et al., 2000). The results do not change if theta frequency is decreased within the 5–10 Hz range typical for rats when the stimulus duration is increased appropriately. Since theta frequency varies linearly with the speed of the animal (Vanderwolf et al., 1977) and presumably duration of excitatory inputs to place cells scales with time spent in the place field, the theta frequency and stimulus duration used in this study represent one instance of dynamically changing, interrelated values.

Background synaptic noise was added to the model cell in the form of randomly fluctuating excitatory and inhibitory conductances injected into the same compartments as the theta

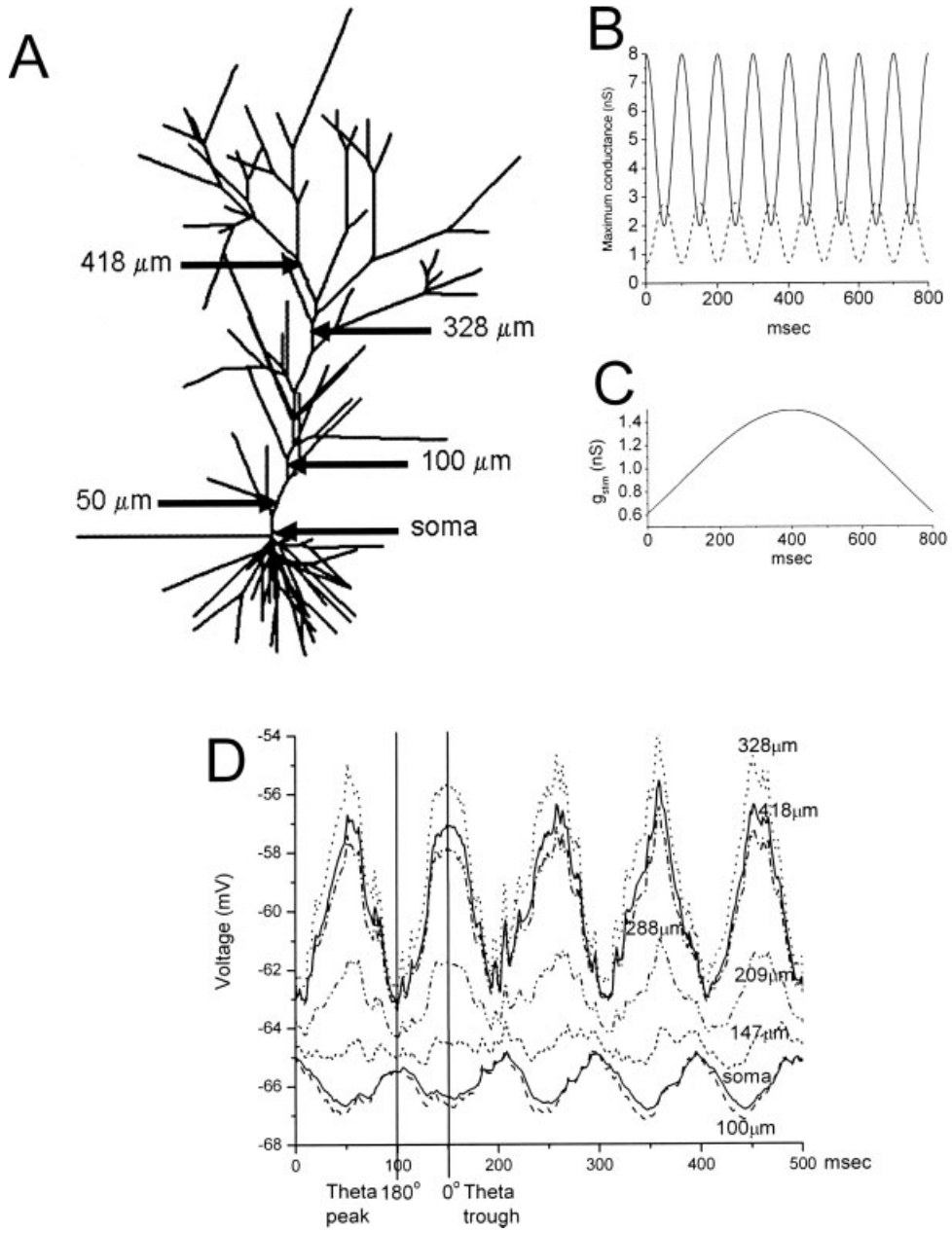

FIGURE 1. A: Schematic of realistic CA1 pyramidal neuron model. B: Theta drive conductances injected to proximal compartment at 100 μm from soma center (solid trace) and to distal compartment at 328 μm from soma center (dashed trace). C: Excitatory Gaussian stimulus conductance injected at various locations. D: Membrane voltage oscillations at various locations along the apical dendrite (distances from soma center indicated) resulting from simulated theta rhythm drive with background synaptic noise present in the model. Phase was measured relative to the proximal theta drive, 0° or 360° is at the hyperpolarizing trough and 180° is at the depolarizing peak.

drives. This noisy synaptic current was modeled as in Destexhe et al. (2001):

$$I_{\text{noise}} = g_e(V - E_e) + g_i(V - E_i)$$

$$dg_e/dt = -g_e/\tau_e + D_e^{1/2}\chi_1(t)$$

$$dg_i/dt = -g_i/\tau_i + D_i^{1/2}\chi_2(t)$$

where $E_e = 0$ mV and $E_i = -80$ mV, $\tau_e = 3$ ms, and $\tau_i = 10$ ms are time constants, D_e and D_i are noise diffusion coefficients, and $\chi_1(t)$ and $\chi_2(t)$ are Gaussian white noise of zero mean and unit standard deviation (SD). We note that τ_i is greater than τ_e to reflect the generally slower decay of inhibitory synaptic currents compared to excitatory synaptic currents. Since these stochastic equations are Gaussian, there is an exact numerical update rule that is independent of the integration

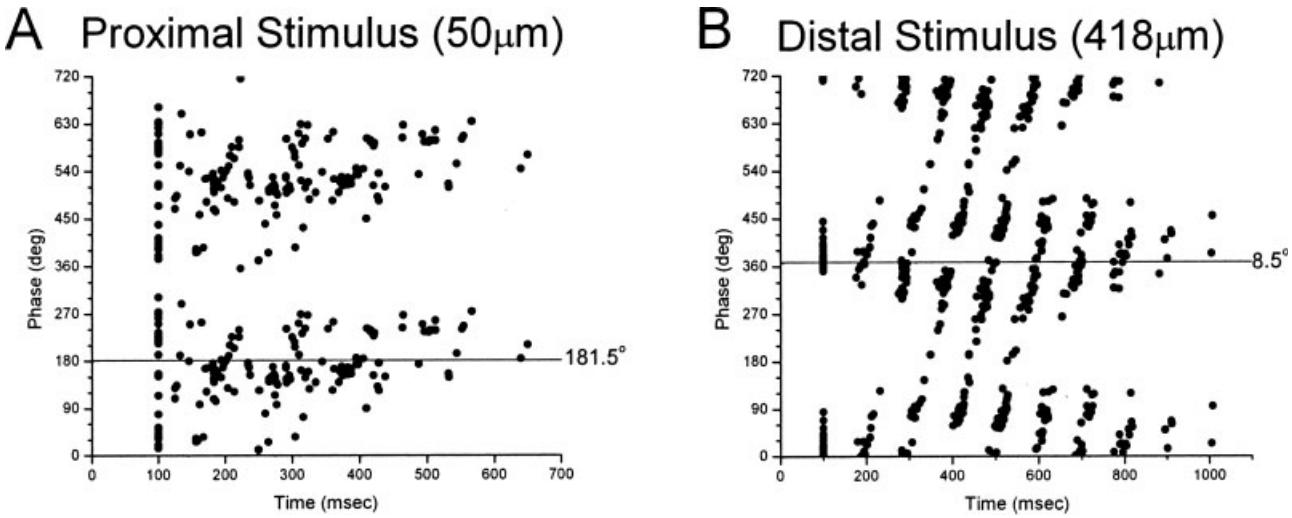

FIGURE 2. Phases of spikes fired in response to a proximal dendritic stimulus (A) (injected 50 μm from soma center, g_{stim} = 1.5 nS) and distal dendritic stimulus (B) (injected 418 μm from soma center, g_{stim} = 1.5 nS) over 50 runs of the model with background synaptic noise present. Spikes fired in each run were aligned so that first spikes occur at 100 ms. Means of mean phases are indicated with the solid horizontal lines.

step h:

$$g_e(t+h) = g_e(t)\exp(-h/\tau_e) + \sigma_e(1-\exp(-2h/\tau_e))^{1/2}N_1(0,1)$$

$$g_i(t+h) = g_i(t)\exp(-h/\tau_i) + \sigma_i(1-\exp(-2h/\tau_i))^{1/2}N_2(0,1)$$

where $\sigma_e = (D_e\tau_e/2)^{1/2}$ and $\sigma_i = (D_i\tau_i/2)^{1/2}$ represent the variances of g_e and g_i, respectively, and $N_1(0,1)$ and $N_2(0,1)$ are normal random numbers of zero mean and unit SD. The variances were set to $\sigma_e = \sigma_i = 0.1$ nS for the noise injected to the proximal compartment (100 μm from soma center) and $\sigma_e = \sigma_i = 0.5$ nS for the noise injected distally (328 μm from soma center). For the results in Figures 3–7, all variances were set to zero.

The theta drive conductances and background synaptic noise produced noisy sinusoidal oscillations in the membrane potential varying over about 1.5 mV at the soma around a mean potential near −66 mV and, in the distal dendrites at 418 μm from soma center, varying over about 6 mV around a mean potential near −60 mV (Fig. 1D). The overall hyperpolarization at the soma and depolarization at the distal dendrites (relative to resting potential at −65 mV) as well as the amplitude and phase differential of the subthreshold oscillations induced by the theta drive agreed with the experimental observations of Kamondi et al. (1998). They reported theta-induced hyperpolarization levels between 2 and 10 mV below the resting membrane potential at the soma and depolarization in the distal dendrites between 2 and 12 mV above resting membrane potential. Amplitudes of theta-induced voltage fluctuations were reported between 2 and 9.5 mV. In our model cell, dendritic membrane potentials proximal to the distal site of theta drive injection displayed oscillations of increasingly smaller amplitude; near ~150 μm from the soma, voltage oscillations were minimal. Through this region where voltage oscillations were minimal, the phase of oscillations gradually shifted over the 180° difference between the distal theta drive and the proximal theta drive, as apparent in the membrane voltage trace at 147 μm from the soma shown in Figure 1D. Proximal to this region, membrane potential oscillations smoothly increased in amplitude and cycled in phase with the proximal theta drive. The distribution in voltage oscillations changed with amplitude of the theta drive conductances (see Results).

We measured phase with respect to the proximal theta drive and defined the peak and trough of the theta cycle by the response of the somatic membrane potential. Specifically, 0° (or 360°) was set at the trough of the somatic membrane potential and 180° was set to its depolarized peak (Fig. 1D).

We modeled generic, excitatory synaptic input by injecting a Gaussian-shaped excitatory conductance (Fig. 1C) to the cell with the form: $I_{stim} = g_{stim}\,(\exp(-(t-t_0)^2/(2\tau^2))\,(V-E_{stim})$, where $E_{stim} = 0$ mV and values of peak conductance g_{stim} are given in the figure captions. The stimulus lasted several hundred milliseconds (τ = 300 ms) and was centered at 400 ms (t_0 = 400 ms for Figs. 1 and 3A–C), 500 ms (t_0 = 500 ms for Fig. 3D–F) or 600 ms (t_0 = 600 ms for Figs. 2, 5–8).

RESULTS

As described in the Model section, we use a CA1 pyramidal cell model that contains a number of realistic features, such as a physiologically accurate dendritic morphology, a variety of

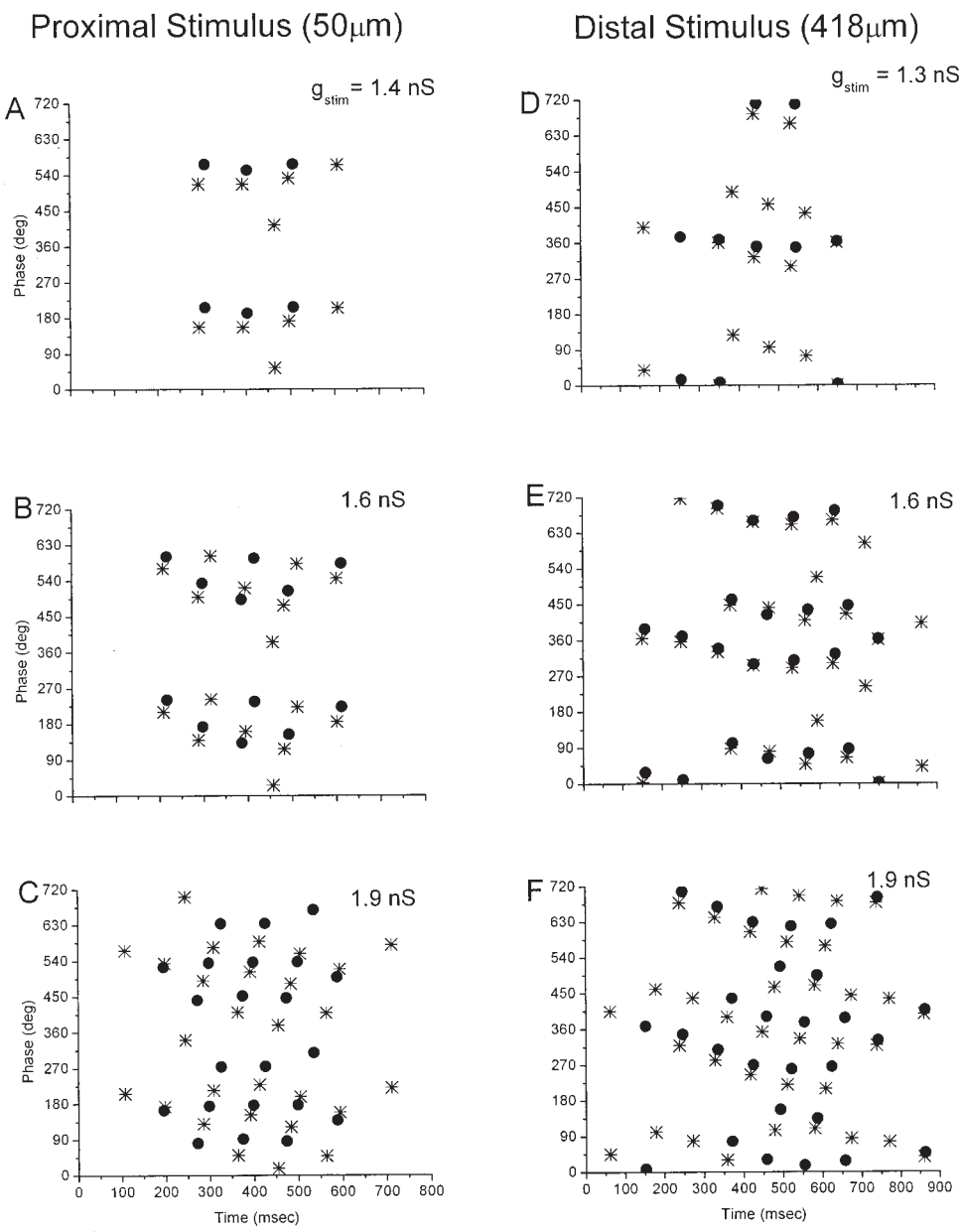

FIGURE 3. Phases of spikes fired in response to stimuli of varying amplitude g_{stim} injected at a proximal dendritic location (A–C) (at 50 μm from soma center) and at a distal dendritic location (D–F) (at 418 μm from soma center) when background synaptic noise was present in the model (asterisks) and when it was absent (filled circles). For the deterministic model results, theta peak and theta trough phase preferences were statistically significant for small and moderate values of g_{stim} (A,B,D,E) (Rayleigh test $P < 0.5$) but not for large g_{stim} values (C and F).

distributed, active ionic currents normally found in these cells, and background synaptic noise. While inclusion of these features complicates the model, it illustrates that our results on the influence of input location on firing phase are not qualitatively affected by such realistic features. The model does remain simple enough to allow for a thorough understanding of the important factors generating these results. For the more detailed analysis of these factors, we consider the model when the background synaptic noise is absent and the model results are deterministic (Figs. 3–7).

Proximal Stimuli Invoked Theta Peak Firing and Distal Stimuli Invoked Theta Trough Firing

When single stimuli were injected at either proximal or distal dendritic sites, a statistically significant preference in firing phase was obtained. Figure 2 shows firing phases in response to either a proximal stimulus (at 50 μm from soma center, Fig. 2A) or a distal stimulus (at 418 μm from soma center, Fig. 2B) for 50 runs of the model with a moderate stimulus amplitude ($g_{stim} = 1.5$ nS). The proximal stimulus invoked firing with a significant phase prefer-

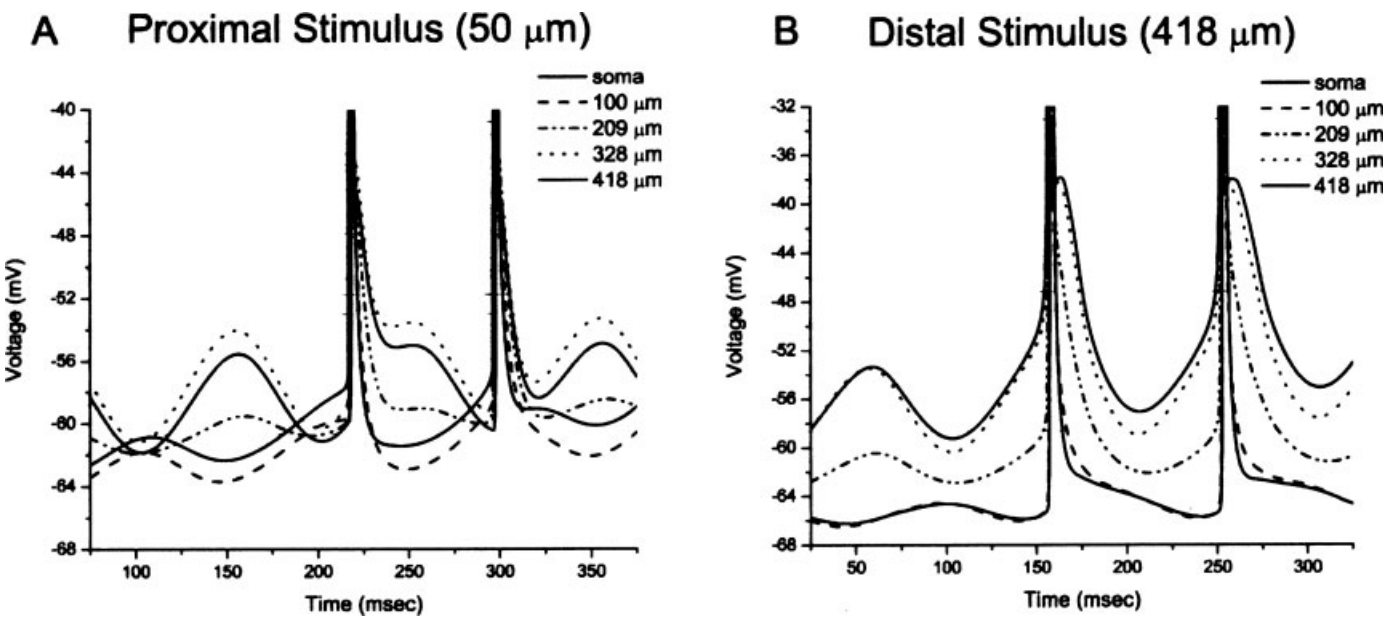

FIGURE 4. Voltage traces at the soma and at various dendritic locations in response to a proximal stimulus (A) (injected at 50 μm from soma center, g_{stim} = 1.6 nS, as in Fig. 3B) and to a distal stimulus (B) (injected at 418 μm from soma center, g_{stim} = 1.6 nS, as in Fig. 3E) in the deterministic model. A: Action potentials are initiated at the soma and axon at theta peaks in response to the proximal stimulus. B: In response to the distal stimulus, action potentials are initiated by propagating dendritic spikes; note that the back-propagation of the action potential leads to an extended dendritic depolarization.

ence near the peak of the somatic theta cycle (mean of means 181.5°, Moore test for uniform phase distribution $P < 0.05$ (Zar, 1999)). In contrast, in response to the distal stimulus, firing showed a significant phase preference in the somatic theta troughs (mean of means 8.5°, Moore test $P < 0.05$). The ∼180° phase difference between the means of means of the distal runs and the proximal runs was also statistically significant (two-sample, 2nd-order test for difference in means $P < 0.05$ (Zar, 1999)).

We note that a slight phase precession of leading spikes over a number of theta cycles can be detected, especially in the firing in response to the distal stimulus (Fig. 2B). This precession is due to the interaction of the theta-induced, subthreshold voltage oscillations in the cell and the increasing amplitude of the distally-injected, Gaussian-shaped stimulus, as predicted by Mehta et al. (2002) and Harris et al. (2002). This slight precession is followed by a slight recession because of the symmetry of the stimulus (see Discussion).

As expected, the amplitude of the stimulus can affect the significance of the phase preference for different input locations. In Figure 3, firing phases for single runs of the model in response to proximal and distal dendritic locations of the stimulus are shown for different stimulus amplitudes when synaptic noise was included (asterisks) and when it was absent (filled circles) from the model. Small amplitude stimuli generated one or two spikes on a number of theta cycles with preferred phases near the somatic theta peak when the stimulus was proximal (Fig. 3A, circular mean 201.7° for deterministic model, Rayleigh test $P < 0.05$ (Batschelet, 1981; Zar, 1999)), and near the theta trough when the stimulus was distal (Fig. 3D, circular mean 1.0° for deterministic model, Rayleigh test $P < 0.05$). For intermediate amplitude stimuli, firing occurred over larger ranges of phases, but phase distributions continued to show a statistically significant preference near the theta peak for proximal input (Fig. 3B, circular mean 193.9° for deterministic model, Rayleigh test $P < 0.05$) and near the theta trough for distal input (Fig. 3E, circular mean 17.3° for deterministic model, Rayleigh test $P < 0.05$). The ∼180° difference in mean firing phases invoked by these proximal and distal stimuli was also measured to be significant (Watson–Williams test $P < 0.05$ (Zar, 1999)). As the stimulus amplitude was increased further, the theta drive did not strongly modulate firing phase, whether the stimulus arrived at either the distal or proximal location (Fig. 3C,F). Action potentials occurred over larger ranges of phases and phase distributions were no different than random (Rayleigh test $P > 0.05$). However, the ∼180° difference in mean phases between distally-invoked and proximally-invoked firing (357.5° and 160.1°, respectively) in the deterministic model was still significant (Watson–Williams test $P < 0.05$).

Why Phase Preference Exists

Important factors underlying this firing phase preference and its dependence on input location were the difference in the phase of the theta drive to proximal and distal regions of the cell, the electrotonic length of the dendritic process, and the presence of active ionic conductances in the dendrites of the cell. Indeed, if the apical dendrites were electrically passive, all firing would occur at the theta peaks. For example, in response to the generic, Gaussian-shaped excitatory stimulus injected at a distal location, the long-lasting excitation would passively propagate and depolarize the proximal regions of the cell. Firing threshold would be first reached at the peaks of the proximal subthres-

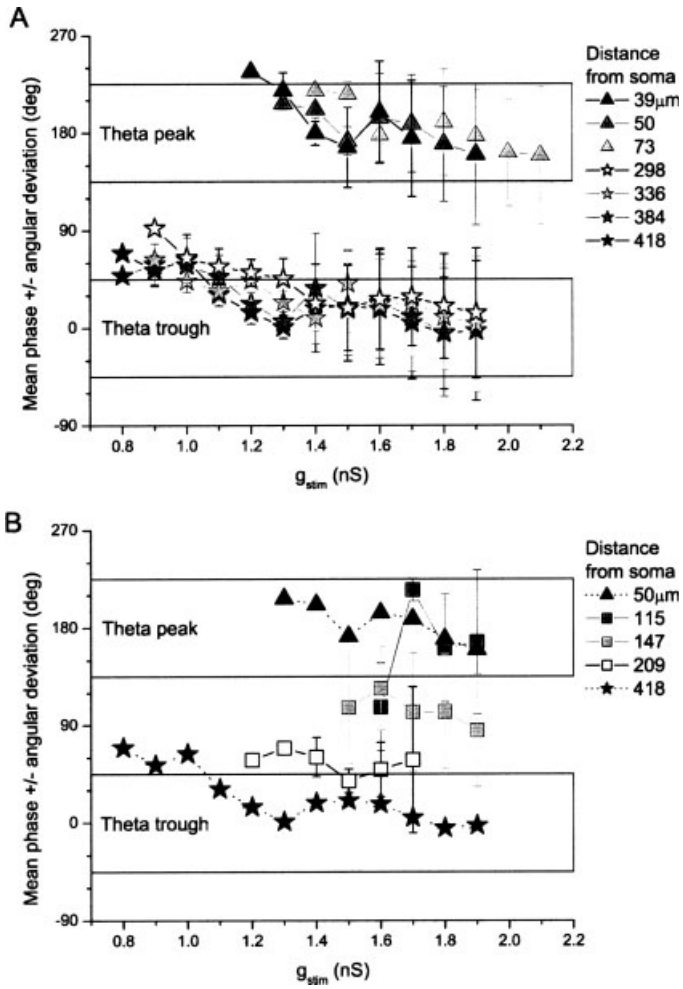

FIGURE 5. A,B: Circular mean phases and angular deviations for spikes fired in response to stimuli of varying maximum amplitude g_{stim} injected at varying locations along apical dendritic shaft in the deterministic model. All but the largest g_{stim} values shown for all locations invoked firing with a statistically significant phase preference (see text). A: Stimuli at distal dendritic locations (distal from 290 μm from soma center, stars) invoked firing with means near the theta trough. Stimuli at proximal dendritic locations (proximal to 100 μm from soma center, triangles) invoked firing with means near the theta peak. B: Stimuli at intermediate dendritic locations (between 100 and 290 μm from soma center, squares) generated firing with means between theta peak and trough. Firing phase means for stimuli at 50 (B, black triangles) and 418 (B, black stars) μm and 90° bands centered at the theta peak and trough (A, B) are shown for reference.

hold oscillation, causing theta peak firing to occur. In the model, however, there are Na^+ and K^+ conductances all along the main apical dendritic shaft out to 500 μm distal from soma center and in the majority of primary and secondary branches out to that same distance. While not present at the same maximal conductance levels as in the short model axon, dendritic Na^+ and K^+ conductances are capable of generating depolarizing spikes that locally depolarize membrane potentials to ~0 mV. In response to an excitatory stimulus, it is clear that spikes—either dendritic or at the soma and axon—will occur preferentially at the peaks of the subthreshold oscillations. Thus, a proximal stimulus depolarizes membrane potentials at the soma and axon that are then pushed across threshold at the peaks of the somatic subthreshold oscillation. Voltage traces at different locations along the main apical dendritic shaft are shown in Figure 4A for the initial spikes in Figure 3B (g_{stim} = 1.6 nS injected at 50 μm from soma center). The action potentials are initiated at the soma at the peak of the somatic theta cycle and then backpropagate into the dendrites. On the other hand, in response to a distal stimulus, dendritic spikes are initiated at the peaks of the dendritic subthreshold oscillation and propagate toward the soma generating a full action potential at the axon (Fig. 4B, g_{stim} = 1.6 nS injected at 418 μm from soma center as in Fig. 3E). The peak of the dendritic oscillation occurs roughly at the trough of the somatic theta cycle; hence the firing phase is near the theta trough.

Proximal and distal dendritic regions of the cell need to be electrotonically distant in order for the distal dendritic membrane to depolarize enough to invoke a dendritic spike while somatic and axonal membrane potentials remain below threshold. As shown in Figure 4B, the somatic and proximal voltages in this model do not rise much above resting potential in response to a distal stimulus. In an electrotonically shorter model cell with similar theta drive conductances but a dendritic process only 200 μm in length, an excitatory stimulus injected at the distal end was able to depolarize the somatic and axonal membrane potentials so that inward currents there were activated at the peaks of the somatic theta cycle and the cell spiked (results not shown). In this shorter model cell, phase was not modulated by the location

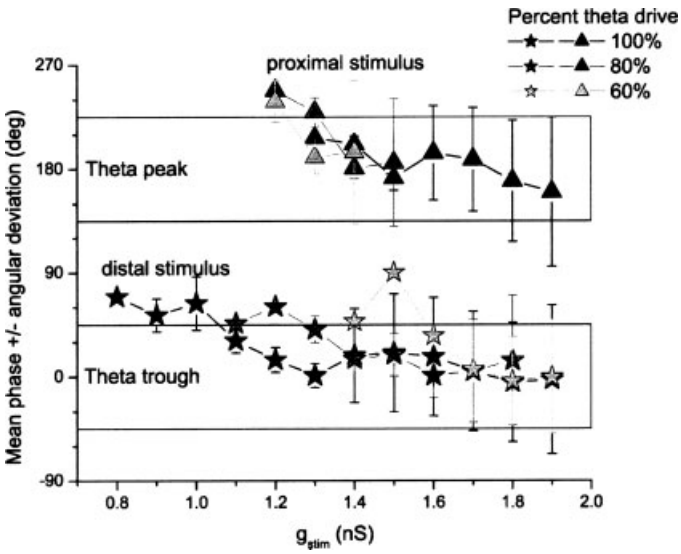

FIGURE 6. Circular mean phases and angular deviations for firing in response to proximal stimuli (injected at 50 μm from soma center, triangles) and distal stimuli (injected at 418 μm from soma center, stars) of varying maximum amplitudes g_{stim} when the maximal conductances of the theta rhythm drives to the cell were reduced to 80% (gray) and 60% (light gray) of their default (100%, black) values in the deterministic model. All but the largest g_{stim} values shown invoked firing with a statistically significant phase preference.

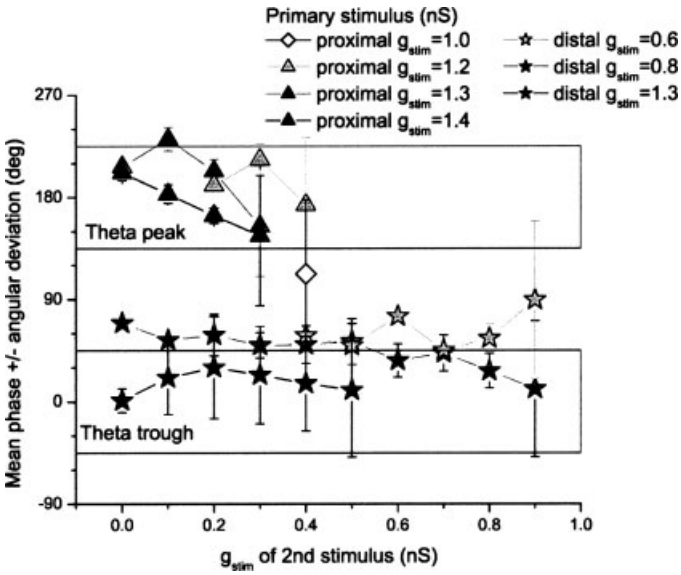

FIGURE 7. Circular mean phases and angular deviations for firing in response to simultaneously injected proximal dendritic (at 50 μm) and distal dendritic (at 418 μm) stimuli in the deterministic model. Amplitudes of larger, primary stimuli were held fixed (values indicated in legend) while amplitudes of smaller, secondary stimuli were varied (values along *x*-axis). All stimulus combinations invoked firing with a statistically significant phase preference except for the largest secondary g_{stim} values shown.

of the stimulus and firing always occurred near the peaks of the somatic theta cycle (see Discussion).

Constraining Factors on the Influence of Input Location on Firing Phase

When the input location was varied along the apical dendritic tree, significant phase preferences in the theta peak and trough were obtained over a range of distances from the soma center (Fig. 5A). In the figure, circular means and angular deviations are shown for firing in response to single stimuli of increasing amplitude g_{stim} that were injected at various locations along the apical dendrite in the deterministic model. When stimuli were located at sites more distal than 290 μm from soma center (stars), mean firing phases were reliably near the theta trough and did not differ significantly across stimulus amplitudes or across these distal sites (Watson–Williams test $P < 0.05$). For stimulus injection sites proximal to 100 μm from soma center (triangles), mean phases clustered near the theta peak and again did not differ significantly across stimulus amplitudes or these proximal sites. However, there was a significant difference between mean firing phases invoked from the distal and proximal sites (Watson–Williams test $P > 0.05$). Significance of phase preference is lost at these ranges of input locations only when the stimulus amplitude becomes too large. For the largest g_{stim} values shown in the figure (and for all larger g_{stim} values not shown), phase distributions were no different from random.

Note that spikes in response to small amplitude distal stimuli occur late in the theta trough. This later firing reflects the later phase of the peaks of the theta-induced subthreshold oscillations in the distal dendrites when the stimulus amplitude is small. In this case, the small stimulus pushes peak voltage levels to near the activation threshold of the dendritic Na^+ currents and not beyond the inactivation threshold of I_A. The interplay of these two competing currents causes a slow depolarization that delays the hyperpolarization phase of the oscillation. For example, for a stimulus amplitude just below firing threshold ($g_{stim} = 0.7$ nS), the oscillation peaks of the distal dendritic membrane potential occur on average 10 ms or 36° after the peak of the distal theta conductance. When stimulus amplitudes are larger, peak voltage levels are pushed well beyond this threshold region such that oscillation peaks, and thus spikes, occur closer to 0°. Spikes in response to small amplitude proximal stimuli do not display late phases but occur closer to the theta peak because the higher density of Na^+ channels and lower conductance levels of I_A in the axon, soma, and proximal dendrites do not allow voltage levels to linger in the threshold region.

When stimuli were injected at locations roughly between 100 and 290 μm from soma center, spikes occurred near both the theta peak and trough, yielding mean phases between the two (Fig. 5B). At these intermediate input locations, the spike initiation site often alternated between somatic initiation by direct depolarization of axonal membrane potentials past threshold, and distal initiation via a propagating dendritic spike. For example, when a stimulus was injected relatively proximally (at 115 μm from soma center, dark gray squares), the majority of spikes generated for a range of stimulus amplitudes were initiated somatically and had phases near the soma theta peaks. But as the stimulus amplitude increased, action potentials were also initiated distally with phases closer to the troughs leading to an overall loss of phase preference. A change in action potential initiation site was responsible for the large increase in mean phase when g_{stim} was increased from 1.6 to 1.7 nS. At 1.6 nS, two action potentials were elicited on one theta cycle, the first initiated distally and the second somatically, leading to a mean phase close to 90° (simulation results not explicitly shown). At 1.7 nS, single spikes were invoked on two consecutive theta cycles and both were initiated somatically, yielding a mean phase closer to 180°. Alternation in spike initiation site also kept mean phases out of the theta trough when the stimulus was injected slightly more distally, at 209 μm from soma center (open squares). Here, for larger stimulus amplitudes, spikes were fired within single theta cycles at the theta peak and at the theta trough with the initiation site alternating between the axon and the distal dendrites. We note that no theta phase precession was observed from spikes generated by inputs at these intermediate sites, unlike the slight phase precession present when action potentials across several theta cycles are all initiated at the same site (as in Fig. 3).

As discussed earlier, one of the underlying mechanisms varying the firing phase preference with input location is the difference in the theta drive to the proximal and distal portions of the cell. Not surprisingly, changes in the theta-induced subthreshold voltage oscillations in the cell affect the significance of firing phase preference. When the maximum conductances of the theta

drives were reduced to 80% and 60% of their original values, the phase preference for proximal and distal stimuli was still present, but significant only in smaller stimulus amplitude ranges (Fig. 6). For a proximal stimulus location (at 50 μm, dark and light gray triangles in Fig. 6), theta peak firing was invoked for small stimulus amplitudes because proximal parts of the cell were less hyperpolarized by a weaker theta drive. The weaker theta drive could not, however, constrain firing to near the theta peak when the amplitude of the stimulus increased. For example, when the maximum conductances of both the proximal and distal theta drive were reduced to 60% of their default values (proximal maximal conductance varied between 4.8 and 1.2 nS, and distal maximal conductance varied between 1.68 and 0.42 nS), the resulting subthreshold membrane potential oscillations at the soma varied over less than 1 mV centered around −66 mV (compared to variation over 1.5 mV with 100% theta drive). These shallow oscillations could not strongly inhibit firing during the theta trough. As a result, within single theta cycles, repetitive firing occurred at low frequencies with subsequent spikes occurring well past the theta peak (as evidenced by the large angular deviations in phase for moderate g_{stim} values). For a distal stimulus location (at 418 μm, dark and light gray stars in Fig. 6), larger amplitude stimuli were necessary to invoke firing than in the original case because distal dendritic voltages were less depolarized by the weaker theta drive. Although a theta trough phase preference remained significant for similar stimulus amplitudes as in the default case, fewer spikes were fired over larger ranges of phases when the theta drive was weaker. Similar to the case for a proximal stimulus location, the theta-induced membrane potential oscillations in the distal dendrites were shallower (voltage varied over less than 4 mV centered near −62 mV compared to 6 mV variation around −60 mV with 100% theta drive) and they could not constrain firing to the distal dendritic oscillation peak (somatic theta trough). Thus, the theta-induced membrane potential oscillations need to be of sufficient amplitude to enforce dendritic or somatic spike initiation at the local oscillation peaks for a range of small to moderate stimulus amplitudes.

Phase Dependence on Location Was Preserved With Simultaneous Distal and Proximal Stimuli

When a proximal stimulus (at 50 μm) and a distal stimulus (at 418 μm) were injected simultaneously, the presence of the second stimulus generally led to an overall increase in depolarization of cell membrane along the entire length of the cell. When the second stimulus was small relative to the larger primary stimulus, this depolarization facilitated an increase in firing in response to the primary stimulus and the phase preference reflected that of the primary stimulus. But when the stimulus amplitudes were less disparate, the combined depolarizing effect of both stimuli led to initiation of action potentials both somatically and distally, and a significant phase preference was not always displayed. In Figure 7, mean phases and angular deviations are plotted for firing induced by simultaneously injected proximal and distal stimuli when the amplitude of the primary stimulus was held fixed (values given in the legend) and the amplitude of the secondary stimulus was increased (values on the *x*-axis). As in previous figures, the largest shown g_{stim} values of the secondary stimulus invoked firing without a significant phase preference.

When the proximal stimulus was the larger primary stimulus (triangles in Fig. 7) and very small amplitude distal stimuli were simultaneously injected, firing phases remained on the theta peak but mean phases decreased due to the overall higher depolarization of the cell that pushed voltages across threshold at earlier phases of the subthreshold oscillation. For slightly larger distal stimuli, significance of the phase preference was lost by the appearance of distally-initiated action potentials near the theta trough on the same theta cycles as somatically-initiated, theta peak spikes. Similar results were obtained when the distal stimulus was the larger primary stimulus (stars in Fig. 7). Smaller amplitudes of the primary distal stimulus (dark and light gray stars) invoked firing with mean phases late in the theta trough for the same reason as outlined in Figure 5A.

When both the proximal and distal stimuli had smaller, less disparate amplitudes, one stimulus was not able to dominate firing and enforce a phase preference (diamond in Fig. 7). The combined depolarizing effect of both stimuli led to action potential initiation both somatically and distally, resulting in spikes near the theta peak and trough and no significant phase preference. These results are similar to how both theta peak and trough spikes were initiated when the stimulus was located in the middle region of the dendrite (Fig. 5B).

Prediction of the Model: Mean Theta Phase Shift in REM Sleep With Experience

Our simulation results suggest that, over the course of familiarization (learning), the shift in mean theta phase of place cell firing during REM (Poe et al., 2000) could occur due to changes in the relative strengths of the proximal SC-CA1 synapses and the distal TA-CA1 synapses. In vivo, activity in the EC would result in activity in both synaptic pathways to CA1. Thus, we assume that CA1 place cells receive input at both the proximal and distal sites. The model simulations in Figure 7 indicate that simultaneously injected proximal and distal stimuli can enforce mean firing phases at the theta peak when the proximal input is stronger relative to the distal input, but generate mean firing phases in the theta trough when the distal input is stronger than the proximal input. A systematic shift in mean phase from theta peak to theta trough may then be achieved through a strengthening of the distal synaptic input and a weakening of the proximal input.

To investigate this prediction in a more robust way, we considered the firing of the model, with background synaptic noise present, in response to proximal stimuli of fixed amplitude and simultaneously injected distal stimuli of increasing amplitude. In Figure 8, the mean of mean firing phases are shown from 50 runs of the model in response to combinations of proximal and distal stimuli. As in previous figures, firing invoked by all but the largest g_{stim} values shown displayed a significant phase preference (Moore test $P < 0.05$). Mean phases were reliably near the theta peak when the proximal stimulus was strong

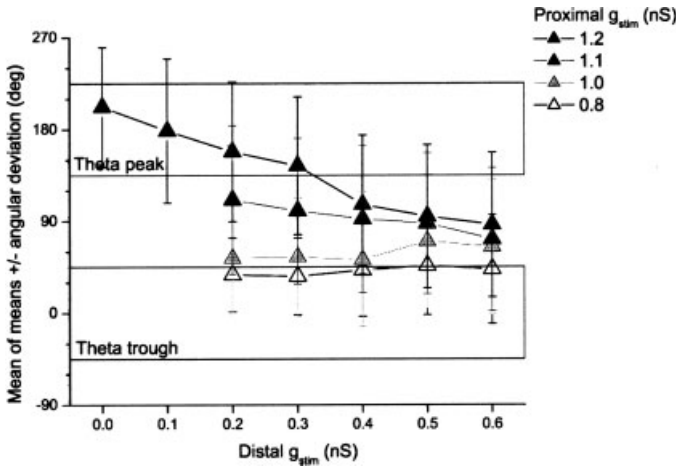

FIGURE 8. Means of mean phases and angular deviations for firing in response to simultaneously injected proximal (at 50 μm) and distal (at 418 μm) stimuli, calculated from 50 simulation runs of the model with background synaptic noise present. Amplitudes of proximal stimuli were held fixed (g_{stim} values in legend) while g_{stim} values for distal stimuli were varied. All but the largest g_{stim} values shown for all stimulus combinations invoked firing with a statistically significant phase preference.

(g_{stim} = 1.2 nS, black triangles) and the distal stimulus was much weaker (0 < distal g_{stim} < 0.2 nS). To obtain mean phases reliably near the theta trough, the proximal stimulus was progressively weakened (g_{stim} = 0.8 nS, open triangles) and the distal stimulus strengthened (distal g_{stim} = 0.2–0.6 nS).

DISCUSSION

Summary of Major Findings and Comparison of Model Constraints With Cell Physiology

The somato-dendritic differential in the theta rhythm drive to CA1 pyramidal cells can result in a difference in firing phase preference for firing invoked by distally-located and proximally-located synaptic inputs. Our simulation study identified a number of factors that limit this theta influence on firing phase, such as active dendritic conductances, the electrotonic length of the cell, the electrotonic separation of input locations, and the amplitude of theta-induced, subthreshold membrane potential oscillations.

Theta trough firing occurred in response to distal dendritic inputs because dendritic active conductances were able to initiate dendritic spikes that could, in turn, generate full action potentials in the cell. It is well known that dendrites of hippocampal pyramidal cells can generate dendritic spikes (for example, Cragg and Hamlyn (1955), Spencer and Kandel (1961), Wong et al. (1979), and Gillies et al. (2002)) (see review in Kasuga et al. (2003)). More recently it has been determined that propagating dendritic spikes can contribute to action potential generation (Turner et al., 1991; Wong and Stewart, 1992; Spruston et al., 1995; Golding and Spruston, 1998; Kasuga et al., 2003; Gasparini et al., 2004).

The phase preference with input location was also aided by a sufficiently long electrotonic length of the dendritic process that could isolate the depolarization required to initiate a dendritic spike from somatic and axonal membrane potentials. Achieving such a separation would depend on the spatial length of the dendritic process as well as the presence and distribution of active ionic currents. For the ionic current distribution in the model, a sufficient electrotonic length was achieved by a spatial extent of the apical dendrite on the order of 500 μm with ~200 μm separating distal (SLM, TA-CA1) inputs from proximal (SR, SC-CA1) inputs. On average, the span of apical dendritic processes in CA1 pyramidal cells encompassing the SR and SLM layers is 625 μm, with SC-CA1 and TA-CA1 synaptic sites separated by distances in the range of 250–300 μm (Ishizuka et al., 1995). It is possible that neuromodulation of dendritic active conductances could reduce electrotonic separation between the SLM and SR layers and affect the influence of input location on firing phase. An excessive electrotonic length, on the other hand, could result in longer conduction delays between the initiation of the dendritic spike and an action potential at the soma and axon that could affect the preferred firing phase. In the model, conduction delays for a dendritic spike initiated at the most distal site investigated (418 μm from soma center) were less than 2 ms, similar to delays measured in CA1 pyramidal cells in vitro (Kasuga et al., 2003; Gasparini et al., 2004) and in vivo (Kloosterman et al., 2001). To affect firing phases by tens of degrees with a 10 Hz theta rhythm, conduction delays would need to be on the order of 10–15 ms, or 5–8 times the realistically modeled electrotonic length. In larger animals where dendritic trees are larger, theta is also slower (e.g., 4–7 Hz in the cat), necessitating a 10–15 times increase in electrotonic length for a conduction delay to significantly affect theta phase.

In our simulations, amplitudes of theta-induced subthreshold oscillations and the extent of hyperpolarization in the proximal portions of the cell and of depolarization in the distal portions of the cell affected the strength and significance of the phase preference. Our default theta drive conductances induced subthreshold oscillations with amplitudes within the range of intradendritic response to theta reported by Kamondi et al. (1998), which were measured in vivo under urethane anesthesia. The profile of extracellular amplitude and phase of theta with depth through the CA1 layers under urethane anesthesia does not differ significantly from depth profiles measured in other states, including active waking (reviewed in Kowalczyk and Konopacki (2002)). The similarity in depth profiles across conditions in various studies suggests that theta-induced intracellular responses along the extent of the cell will also be similar in different behavioral states of the animal.

Modeling Limitations

In our simulations, both theta drive and synaptic inputs were simplified to point processes injected on the main apical dendritic shaft of the model cell. These simplifications allowed a close investigation of the important factors contributing to the

firing phase preference with input location and of the effects of manipulating those factors. It was the subthreshold voltage oscillations induced by the theta drive that contributed most to the phase preference. We expect that if a physiologically realistic, distributed model of the theta drive was implemented, taking into account rhythmic inhibitory inputs from interneuronal networks and excitatory inputs from the EC (Buzsaki, 2002), such that it invoked similar amplitude subthreshold oscillations with similar differences in proximal hyperpolarization and distal depolarization, a phase preference with input location as found in the present study would also be obtained.

We modeled the synaptic input as a lumped excitatory stimulus entering the cell at a single site. The intent of the generic, Gaussian-shaped stimulus was to represent a pattern of increase and then decrease in the net excitatory input to the cell that would consist of many distributed excitatory synaptic inputs modulated by distributed inhibitory inputs from CA1 interneurons. Physiologically, both distal and proximal inputs to the cell would certainly be distributed processes targeting the cell throughout the dendritic arbor. The important factor for the generation of phase preference, however, was the initiation site of the action potential, either proximally by direct depolarization of membrane potentials in the soma and axon, or distally through a propagating dendritic spike. We expect that if synaptic input were modeled as many small inputs distributed throughout the SR and SLM layers and if the distinction remained between the two types of action potential generation mechanisms, then phase preference with synaptic input location would be maintained.

A Word About Theta Phase Precession

The primary focus of this study was on mechanisms for altering the mean theta phase of firing. However, similar mechanisms have been previously employed to account for phase precession (Kamondi et al., 1998; Magee, 2001; Harris et al., 2002; Huhn et al., 2005). The soma-dendritic interference (SDI) model for phase precession (Kamondi et al., 1998; Magee, 2001; Harris et al., 2002) proposes that the 180° phase differential in the theta rhythm between the soma and distal dendrites can generate a phase advancement of spikes in response to increasing levels of excitation arriving at a single location. Indeed, an initial precession of firing phases is seen in response to the distal stimulus in Figure 2B, although this precession is followed by phase recession due to the symmetry of the excitatory input. In our simulation study, since distal stimuli cause firing in the theta trough and proximal stimuli cause firing near theta peaks, it is not surprising that an initial distal stimulus followed by a proximal stimulus would generate firing across almost all phases (simulations not shown). Indeed, our simulation results, which depend on a sufficiently long spatial extent of the dendritic process and on the electrotonic separation of the excitatory afferent pathways, provide for robust phase advancement over a large range of phases in response to excitatory input that is not temporally patterned. Temporal patterning of inputs may additionally contribute to theta phase precession, but those investigations are beyond the scope of the present study.

Support for Model Prediction: Mean Theta Phase Shift in REM Sleep With Experience

As illustrated in the simulation results of Figure 8, a phase shift from theta peaks to troughs can occur as a result of decreases in the strengths of proximal inputs coupled with increases in distal input strengths. We propose that the theta phase shift during REM replay over several days during learning (Poe et al., 2000) reflects a pattern of synaptic plasticity wherein initially potentiated SC-CA1 synapses depotentiate as TA-CA1 synapses potentiate. Specifically, we propose that theta peak firing during REM replay in the first 2 days of exposure to a novel environment is compatible with potentiated SC-CA1 synapses and still relatively weak TA-CA1 synapses. We further propose that theta trough firing during REM replay after familiarization is consistent with potentiated TA-CA1 synapses and depotentiated SC-CA1 synapses. These hypotheses were derived from simulation results. Physiological studies of brain activity in intact animals are necessary to directly test these hypotheses. However, different lines of experimental evidence in the literature, indirectly support the occurrence of varying synaptic strengths at SC-CA1 and TA-CA1 synapses during familiari zation.

Plasticity at TA-CA1 synapses occurs independently of plasticity at SC-CA1 synapses (Dvorak-Carbone and Schuman, 1999; Remondes and Schuman, 2003) and more powerful stimulation protocols are required to induce long term potentiation (long-term potentiation (LTP)) at TA-CA1 synapses than at SC-CA1 synapses (Dvorak-Carbone and Schuman, 1999; Remondes and Schuman, 2002, 2003). LTP occurs readily through synapses in the trisynaptic loop, particularly during exploration of novel environments (Mehta et al., 1997; Ekstrom et al., 2001; Davis et al., 2004; Nitz and McNaughton, 2004), when place cells fire predominantly at theta peaks, where LTP most readily occurs (Pavlides et al., 1988; Holscher et al., 1997; Orr et al., 2001; Hyman et al., 2003). As a result, SC-CA1 synaptic input would initially dominate CA1 cell response. With repeated exposures to the environment, TA-CA1 synapses would be expected to gradually strengthen.

Synaptic plasticity can also occur in REM sleep with the same types of inputs that induce plasticity in the waking animal (Leonard et al., 1987; Bramham and Srebro, 1989; Ribeiro et al., 1999, 2002). Theta peak firing during REM sleep over the first 2 days of exposure to the novel environment would thus continue to strengthen synapses along the SC-CA1 pathway.

In opposition to the initial SC-CA1 synaptic dominance, the absence of serotonin and norepinephrine in the hippocampus during REM modulates ionic conductances in CA1 pyramidal cells (Aghajanian, 1985; Andrade and Nicoll, 1987; Colino and Halliwell, 1987; Gasparini and DiFrancesco, 1999; Choi et al., 2004) such that the response to distal dendritic synaptic input is amplified relative to proximal inputs (Andrade and Nicoll, 1987; Colino and Halliwell, 1987; Gasparini and DiFrancesco, 1999; Magee, 1999; Takigawa and Alzheimer, 2002; Migliore et al., 2004). Specifically, the effects of I_h become less relevant during REM sleep when serotonin, which boosts I_h currents (Aghajanian, 1985;

Andrade and Nicoll, 1987; Colino and Halliwell, 1987; Gasparini and DiFrancesco, 1999; Choi et al., 2004), is uniquely absent (reviewed in Pace-Schott and Hobson (2002)). Conversely, the distribution of I_A becomes more relevant during REM sleep when serotonin and norepinephrine, both of which inhibit I_A (Aghajanian, 1985; Choi et al., 2004) are absent. Once distal TA-CA1 inputs are potentiated, the shift to theta trough dominated activity would be unmasked during REM.

During waking, despite strengthened TA-CA1 inputs, trough firing may remain occluded when serotonin and norepinephrine return to higher levels. However, depending on the size of the waking serotonin occlusion effect, some trough firing may begin to appear in waking from strengthened distal inputs, perhaps explaining the observation by Yamaguchi et al. (2002) of a locus of firing at theta troughs during phase precession.

Strengthened TA-CA1 synaptic input can lead to depotentiation of SC-CA1 synapses through spike-blocking interneuronal activity (Dvorak-Carbone and Schuman, 1999). TA activation also leads to interneurons releasing depotentiation-enhancing endogenous peptides (Wagner et al., 2001). The depotentiation of synapses during REM is further aided by the absence of hippocampal norepinephrine (Thomas et al., 1996; Katsuki et al., 1997). Moreover, depotentiation of SC-CA1 synapses leads to the disinhibition of TA inputs (Maccaferri and McBain, 1995).

These mechanisms support a change in synaptic strengths at proximal and distal input sites during waking and REM sleep over the course of learning. It has recently been shown that while TA input is not required for recall of short-term spatial memories, it is essential for long-term consolidation of spatial memories (Remondes and Schuman, 2004). A change from SC-dominated to TA-dominated hippocampal cell responses during memory consolidation may underlie the shift in mean theta phase observed in REM replay (Poe et al., 2000). As a consequence, novel experiences would initially play through the trisynaptic circuit and REM sleep would serve a learning support function. After familiarization, experiences would be reactivated more strongly through the TA-CA1 pathway and REM sleep could serve a housekeeping function to clear redundant encoding in SC-CA1 synapses. The results reported in the present simulation study, therefore, suggest a refinement to the putative role of theta trough firing proposed by Poe et al. (2000). Instead of depotentiating all hippocampal synapses involved in encoding familiar and consolidated memories, theta trough firing during REM would weaken only the novelty-related pathway (SC-CA1) while maintaining and perhaps further strengthening the TA-CA1 recognition loop.

REFERENCES

Aghajanian GK. 1985. Modulation of a transient outward current in serotonergic neurones by alpha 1-adrenoceptors. Nature 315:501–503.

Andrade R, Nicoll RA. 1987. Pharmacologically distinct actions of serotonin on single pyramidal neurones of the rat hippocampus recorded in vitro. J Physiol 394:99–124.

Batschelet E. 1981. Circular statistics in biology. London, New York: Academic Press.

Bramham CR, Srebro B. 1989. Synaptic plasticity in the hippocampus is modulated by behavioral state. Brain Res 493:74–86.

Buzsaki G. 2002. Theta oscillations in the hippocampus. Neuron 33:325–340.

Choi JS, Choi BH, Ahn HS, Kim MJ, Han TH, Rhie DJ, Yoon SH, Jo YH, Kim MS, Hahn SJ. 2004. Fluoxetine inhibits A-type potassium currents in primary cultured rat hippocampal neurons. Brain Res 1018:201–207.

Colino A, Halliwell JV. 1987. Differential modulation of three separate K-conductances in hippocampal CA1 neurons by serotonin. Nature 328:73–77.

Cragg BG, Hamlyn LH. 1955. Action potentials of the pyramidal neurons in the hippocampus of the rabbit. J Physiol 129:608–627.

Davis CD, Jones FL, Derrick BE. 2004. Novel environments enhance the induction and maintenance of long-term potentiation in the dentate gyrus. J Neurosci 24:6497–6506.

Destexhe A, Rudolph M, Fellous J-M, Sejnowski TJ. 2001. Fluctuating synaptic conductances recreate in vivo-like activity in neocortical neurons. Neuroscience 107:13–24.

Dvorak-Carbone H, Schuman EM. 1999. Long-term depression of temporoammonic-CA1 hippocampal synaptic transmission. J Neurophysiol 81:1036–1044.

Ekstrom AD, Meltzer J, McNaughton BL, Barnes CA. 2001. NMDA receptor antagonism blocks experience-dependent expansion of hippocampal "place fields". Neuron 31:631–638.

Gasparini S, DiFrancesco D. 1999. Action of serotonin on the hyperpolarization-activated cation current (Ih) in rat CA1 hippocampal neurons. Eur J Neurosci 11:3093–3100.

Gasparini S, Migliore M, Magee JC. 2004. On the initiation and propagation of dendritic spikes in CA1 pyramidal neurons. J Neurosci 24:11046–11056.

Gillies MJ, Traub RD, LeBeau FE, Davies CH, Gloveli T, Buhl EH, Whittington MA. 2002. A model of atropine-resistant theta oscillations in rat hippocampal area CA1. J Physiol 543(Pt 3):779–793.

Givens B. 1996. Stimulus-evoked resetting of the dentate theta rhythm: relation to working memory. Neuroreport 8:159–163.

Golding NL, Spruston N. 1998. Dendritic sodium spikes are variable triggers of axonal action potentials in hippocampal CA1 pyramidal neurons. Neuron 21:1189–1200.

Harris KD, Henze DA, Hirase H, Leinekugel X, Dragoi G, Czurko A, Buzsaki G. 2002. Spike train dynamics predicts theta-related phase precession in hippocampal pyramidal cells. Nature 417:738–741.

Hines ML, Carnevale NT. 1997. The NEURON simulation environment. Neural Comput 9:1179–1209.

Hobson JA, Pace-Schott EF. 2002. The cognitive neuroscience of sleep: neuronal systems, consciousness and learning. Nat Rev Neurosci 3:679–693.

Holscher C, Anwyl R, Rowan MJ. 1997. Stimulation on the positive phase of hippocampal theta rhythm induces long-term potentiation that can be depotentiated by stimulation on the negative phase in area CA1 in vivo. J Neurosci 17:6470–6477.

Huhn Z, Orban G, Erdi P, Lengyel M. 2005. Theta oscillation-coupled dendritic spiking integrates inputs on a long time scale. Hippocampus 15:950–962.

Hyman JM, Wyble BP, Goyal V, Rossi CA, Hasselmo ME. 2003. Stimulation in hippocampal region CA1 in behaving rats yields long-term potentiation when delivered to the peak of theta and long-term depression when delivered to the trough. J Neurosci 23:11725–11731.

Ishizuka N, Cowan WM, Amaral DG. 1995. A quantitative analysis of the dendritic organization of pyramidal cells in the rat hippocampus. J Comp Neurol 362:17–45.

Kamondi A, Acsady L, Wang XJ, Buzsaki G. 1998. Theta oscillations in somata and dendrites of hippocampal pyramidal cells in vivo: activity-dependent phase-precession of action potentials. Hippocampus 8:244–261.

Kasuga A, Enoki R, Hashimoto Y, Akiyama H, Kawamura Y, Inoue M, Kudo Y, Miyakawa H. 2003. Optical detection of dendritic spike initiation in hippocampal CA1 pyramidal neurons. Neuroscience 118:899–907.

Katsuki H, Izumi Y, Zorumski CF. 1997. Noradrenergic regulation of synaptic plasticity in the hippocampal CA1 region. J Neurophysiol 77:3013–3020.

Kloosterman F, Peloquin P, Leung LS. 2001. Apical and basal orthodromic population spikes in hippocampal CA1 in vivo show different origins and patterns of propagation. J Neurophysiol 86:2435–2444.

Kowalczyk T, Konopacki J. 2002. Depth amplitude and phase profiles of carbachol-induced theta in hippocampal formation slices. Brain Res Bull 58:569–574.

Lee AK, Wilson MA. 2002. Memory of sequential experience in the hippocampus during slow wave sleep. Neuron 36:1183–1194.

Leonard BJ, McNaughton BL, Barnes CA. 1987. Suppression of hippocampal synaptic plasticity during slow-wave sleep. Brain Res 425: 174–177.

Louie K, Wilson MA. 2001. Temporally structured replay of awake hippocampal ensemble activity during rapid eye movement sleep. Neuron 29:145–156.

Maccaferri G, McBain CJ. 1995. Passive propagation of LTD to stratum oriens-alveus inhibitory neurons modulates the temporoammonic input to the hippocampal CA1 region. Neuron 15:137–145.

Magee JC. 1999. Dendritic lh normalizes temporal summation in hippocampal CA1 neurons. Nat Neurosci 2:508–514.

Magee JC. 2001. Dendritic mechanisms of phase precession in hippocampal CA1 pyramidal neurons. J Neurophysiol 86:528–532.

Mehta MR, Barnes CA, McNaughton BL. 1997. Experience-dependent, asymmetric expansion of hippocampal place fields. PNAS 94: 8918–8921.

Mehta MR, Lee AK, Wilson MA. 2002. Role of experience and oscillations in transforming a rate code into a temporal code. Nature 417:741–746.

Migliore M. 2003. On the integration of subthreshold inputs from perforant path and Schaffer collaterals in hippocampal CA1 pyramidal neurons. J Comput Neurosci 14:185–192.

Migliore M, Hoffman DA, Magee JC, Johnston D. 1999. Role of an A-type K+ conductance in the back-propagation of action potentials in the dendrites of hippocampal pyramidal neurons. J Comput Neurosci 7:5–15.

Migliore M, Messineo L, Ferrante M. 2004. Dendritic Ih selectively blocks temporal summation of unsynchronized distal inputs in CA1 pyramidal neurons. J Comput Neurosci 16:5–13.

Mizumori SJ, Perez GM, Alvarado MC, Barnes CA, McNaughton BL. 1990. Reversible inactivation of the medial septum differentially affects two forms of learning in rats. Brain Res 528:12–20.

Nitz D, McNaughton B. 2004. Differential modulation of CA1 and dentate gyrus interneurons during exploration of novel environments. J Neurophysiol 91:863–872.

Orr G, Rao G, Houston FP, McNaughton BL, Barnes CA. 2001. Hippocampal synaptic plasticity is modulated by theta rhythm in the fascia dentata of adult and aged freely behaving rats. Hippocampus 11:647–654.

Pace-Schott EF, Hobson JA. 2002. The neurobiology of sleep: genetics, cellular physiology and subcortical networks. Nat Rev Neurosci 3:591–605.

Pavlides C, Greenstein YJ, Grudman M, Winson J. 1988. Long-term potentiation in the dentate gyrus is induced preferentially on the positive phase of theta-rhythm. Brain Res 439:383–387.

Poe GR, Nitz DA, McNaughton BL, Barnes CA. 2000. Experience-dependent phase-reversal of hippocampal neuron firing during REM sleep. Brain Res 855:176–180.

Poolos NP, Migliore M, Johnston D. 2002. Pharmacological upregulation of h-channels reduces the excitability of pyramidal neuron dendrites. Nat Neurosci 5:767–774.

Rashidy-Pour A, Motamedi F, Motahed-Larijani Z. 1996. Effects of reversible inactivations of the medial septal area on reference and working memory versions of the Morris water maze. Brain Res 709:131–140.

Remondes M, Schuman EM. 2002. Direct cortical input modulates plasticity and spiking in CA1 pyramidal neurons. Nature 416:736–740.

Remondes M, Schuman EM. 2003. Molecular mechanisms contributing to long-lasting synaptic plasticity at the temporoammonic-CA1 synapse. Learn Mem 10:247–252.

Remondes M, Schuman EM. 2004. Role for a cortical input to hippocampal area CA1 in the consolidation of a long-term memory. Nature 431:699–703.

Ribeiro S, Goyal V, Mello CV, Pavlides C. 1999. Brain gene expression during REM sleep depends on prior waking experience. Learn Mem 6:500–508.

Ribeiro S, Mello CV, Velho T, Gardner TJ, Jarvis ED, Pavlides C. 2002. Induction of hippocampal long-term potentiation during waking leads to increased extrahippocampal zif-268 expression during ensuing rapid-eye-movement sleep. J Neurosci 22:10914–10923.

Ribeiro S, Nicolelis MA. 2004. Reverberation, storage, and postsynaptic propagation of memories during sleep. Learn Mem 11:686–696.

Skaggs WE, McNaughton BL. 1996. Replay of neuronal firing sequences in rat hippocampus during sleep following spatial experience. Science 271:1870–1873.

Spencer WA, Kandel ER. 1961. Electrophysiology of hippocampal neurons: IV. Fast prepotentials. J Neurophysiol 24:272–285.

Spruston N, Schiller Y, Stuart G, Sakmann B. 1995. Activity-dependent action potential invasion and calcium influx into hippocampal CA1 dendrites. Science 268:297–300.

Takigawa T, Alzheimer C. 2002. Phasic and tonic attenuation of EPSPs by inward rectifier K+ channels in rat hippocampal pyramidal cells. J Physiol 539(Pt 1):67–75.

Thomas MJ, Moody TD, Makhinson M, O'Dell TJ. 1996. Activity-dependent beta-adrenergic modulation of low frequency stimulation induced LTP in the hippocampal CA1 region. Neuron 17:475–482.

Turner R, Meyers D, Richardson T, Barker J. 1991. The site for initiation of action potential discharge over the somatodendritic axis of rat hippocampal CA1 pyramidal neurons. J Neurosci 11:2270–2280.

Vanderwolf CH, Kramis R, Robinson TE. 1977. Hippocampal electrical activity during waking behaviour and sleep: analyses using centrally acting drugs. Ciba Found Symp 58:199–226.

Wagner JJ, Etemad LR, Thompson AM. 2001. Opioid-mediated facilitation of long-term depression in rat hippocampus. J Pharmacol Exp Ther 296:776–781.

Wilson MA, McNaughton BL. 1994. Reactivation of hippocampal ensemble memories during sleep. Science 265:676–679.

Wong RK, Stewart M. 1992. Different firing patterns generated in dendrites and somata of CA1 pyramidal neurons in guinea-pig hippocampus. J Physiol 457:675–687.

Wong RKS, Prince DA, Basbaum AI. 1979. Intradendritic recordings from hippocampal neurons. PNAS 76:986–990.

Yamaguchi Y, Aota Y, McNaughton BL, Lipa P. 2002. Bimodality of theta phase precession in hippocampal place cells in freely running rats. J Neurophysiol 87:2629–2642.

Zar JH. 1999. Biostatistical analysis. Upper Saddle River, New Jersey: Prentice Hall.